Ratio of the Parametric X-Radiation Yields in the Bragg Direction and along the Relativistic Electron Velocity in the Bragg Geometry

S. V. Blazhevich and A. V. Noskov

Belgorod State University, Belgorod, Russia

Abstract—Parametric X-radiation (PXR) and parametric radiation at a small angle to the relativistic electron velocity (FPXR) that arises from electron motion through a monocrystalline plate in Bragg scattering geometry are analyzed on the basis of the dynamic diffraction theory. The expressions for spectral-angular densities of these radiations have been derived in the general case of asymmetric field reflections from a target surface. They make it possible to reveal the noticeable dependence of the ratio of the PXR and FPXR yields on the angle between reflecting atomic planes and the surface of a monocrystalline plate, i.e., reflection asymmetry.

INTRODUCTION

When a charged particle crosses a monocrystal, pseudophotons of its Coulomb field are scattered by a set of the parallel atomic planes of a crystal, generating parametric X-radiation (PXR) [1–3]. According to the theory of PXR, each photon generated in the Bragg direction must correspond to a photon moving along the emitting particle velocity [4–6]. PXR along the emitting particle velocity (often referred to as forward PXR (FPXR)) is a purely dynamic effect (the manifestation of the effects of dynamic diffraction in PXR). Hence, its features are of great interest for the physics of charged-particle interaction with crystals. Attempts at experimental investigations are known [7–11]. However, this radiation has first been measured in the Laue scattering geometry only in experiment [11]. The desired FPXR reflection was almost indistinguishable against the background of radiation produced by electrons on the structural components of the experimental setup. Thus, theoretical investigations of FPXR properties and searching for conditions ensuring its reliable experimental observation remain very urgent problems.

Detailed theoretical descriptions of the dynamic FPXR effect in the symmetric geometry were reported in [12–14]. In the general case of asymmetric reflections, theoretical descriptions of PXR and FPXR can be found, respectively, in [15–17] and [18, 19]. In these studies, the spectral-angular radiation density was shown to be substantially dependent upon reflection asymmetry for the mentioned mechanisms and effects related to asymmetry were revealed. The ratios of PXR and FPXR yields in the Laue geometry were discussed in [20], where it was found that the ratio of yields can vary cardinally with a change in asymmetry.

In this study, on the basis of the two-wave approximation of dynamic diffraction theory [21], analytical expressions for the PXR and FPXR amplitudes were derived under the general condition of asymmetric reflections and expressions describing the spectral-angular densities of these radiations were obtained. They were used to investigate the dependence of the ratio of yields on reflection asymmetry in the Bragg scattering geometry.

RADIATION AMPLITUDE

It is assumed that a fast charged particle with constant velocity $\mathbf{V}$ crosses a monocrystalline plate in the Bragg scattering geometry (Fig. 1). Let us consider the equations for the Fourier transform of an electromagnetic field:

$$\mathbf{E}(\mathbf{k}, \omega) = \int dt\, d^3\mathbf{r}\, \mathbf{E}(\mathbf{r}, t) \exp(i\omega t - i\mathbf{k}\mathbf{r}). \quad (1)$$

With a high degree of accuracy, a relativistic particle field can be assumed to be transverse. Therefore, incident $\mathbf{E}_0(\mathbf{k}, \omega)$ and diffracted $\mathbf{E}_\mathbf{g}(\mathbf{k}, \omega)$ electromagnetic waves is defined by two amplitudes with different values of transverse polarizations:

$$\begin{aligned} \mathbf{E}_0(\mathbf{k}, \omega) &= E_0^{(1)}(\mathbf{k}, \omega)\mathbf{e}_0^{(1)} + E_0^{(2)}(\mathbf{k}, \omega)\mathbf{e}_0^{(2)}, \\ \mathbf{E}_\mathbf{g}(\mathbf{k}, \omega) &= E_\mathbf{g}^{(1)}(\mathbf{k}, \omega)\mathbf{e}_1^{(1)} + E_\mathbf{g}^{(2)}(\mathbf{k}, \omega)\mathbf{e}_1^{(2)}, \end{aligned} \quad (2)$$

where unit vectors $\mathbf{e}_0^{(1)}$ and $\mathbf{e}_0^{(2)}$ are perpendicular to vector $\mathbf{k}$ and unit vectors $\mathbf{e}_1^{(1)}$ and $\mathbf{e}_1^{(2)}$ are perpendicular to the vector $\mathbf{k}_\mathbf{g} = \mathbf{k} + \mathbf{g}$. In addition, vectors $\mathbf{e}_0^{(2)}$ and $\mathbf{e}_1^{(2)}$ lie in the plane of vectors $\mathbf{k}$ and $\mathbf{k}_\mathbf{g}$ (π polarization), vectors $\mathbf{e}_0^{(1)}$ and $\mathbf{e}_1^{(1)}$ are perpendicular to this plane (σ polarization), and reciprocal lattice vector $\mathbf{g}$ defines a set of reflecting atomic planes in the crystal. In the two-wave approximation of the dynamic theory of diffraction, the system of equations describing the

Fourier transform of an electromagnetic field is written as [22]

$$\begin{cases} (\omega^2(1+\chi_0)-k^2)E_0^{(s)} + \omega^2\chi_{-\mathbf{g}}C^{(s,\tau)}E_{\mathbf{g}}^{(s)} \\ = 8\pi^2 ie\omega\theta VP^{(s)}\delta(\omega-\mathbf{kV}), \\ \omega^2\chi_{\mathbf{g}}C^{(s,\tau)}E_0^{(s)} + (\omega^2(1+\chi_0)-k_{\mathbf{g}}^2)E_{\mathbf{g}}^{(s)} = 0, \end{cases} \tag{3}$$

where $\chi_0 = \chi_0' + i\chi_0''$ is the average dielectric susceptibility of a crystal and $\chi_{\mathbf{g}}$ and $\chi_{-\mathbf{g}}$ are the Fourier coefficients of expansion of the dielectric susceptibility in terms of reciprocal lattice vectors **g**:

$$\begin{aligned} \chi(\omega, \mathbf{r}) &= \sum_{\mathbf{g}} \chi_{\mathbf{g}}(\omega)\exp i\mathbf{gr} \\ &= \sum_{\mathbf{g}} \left(\chi_{\mathbf{g}}'(\omega) + i\chi_{\mathbf{g}}''(\omega)\right)\exp i\mathbf{gr}. \end{aligned} \tag{4}$$

Let us consider a crystal with central symmetry ($\chi_{\mathbf{g}} = \chi_{-\mathbf{g}}$). Quantities $\chi_{\mathbf{g}}'$ and $\chi_{\mathbf{g}}''$ in (4) are defined as

$$\begin{aligned} \chi_{\mathbf{g}}' &= \chi_0'(F(g)/Z)(S(\mathbf{g})/N_0)\exp\left(-\frac{1}{2}g^2u_\tau^2\right), \\ \chi_{\mathbf{g}}'' &= \chi_0''\exp\left(-\frac{1}{2}g^2u_\tau^2\right), \end{aligned} \tag{5}$$

Here, $F(g)$ is the form factor of an atom containing Z electrons, $S(\mathbf{g})$ is the structure factor of an elementary cell containing N_0 atoms, and u_τ is the rms amplitude of thermal oscillations of atoms in the crystal. In this paper, we are concerned with the X-ray frequency range, in which $\chi_{\mathbf{g}}' < 0$ and $\chi_0' < 0$.

In system (3), quantities $C^{(s,\tau)}$ and $P^{(s)}$ are defined as

$$\begin{aligned} C^{(s,\tau)} &= \mathbf{e}_0^{(s)}\mathbf{e}_1^{(s)} = (-1)^\tau C^{(s)}, \quad C^{(1)} = 1, \quad C^{(2)} = |\cos 2\theta_B|, \\ P^{(s)} &= \mathbf{e}_0^{(s)}(\boldsymbol{\mu}/\mu), \quad P^{(1)} = \sin\varphi, \quad P^{(2)} = \cos\varphi, \end{aligned} \tag{6}$$

Here, $\boldsymbol{\mu} = \mathbf{k} - \omega\mathbf{V}/V^2$ is the virtual-photon momentum component perpendicular to particle velocity **V** ($\mu = \omega\theta/V$, where $\theta \ll 1$ is the angle between **k** and **V**), θ_B is the angle between the electron velocity and a set of crystallographic planes (the Bragg angle), and φ is the azimuthal angle of radiation (its value is counted off from the plane formed by vectors **V** and **g**). The value of the reciprocal lattice vector is determined by the expression $g = 2\omega_B \sin\theta_B/V$, where ω_B is the Bragg frequency. System (3) describes s-polarized fields if $s = 1$ and $\tau = 2$ and σ-polarized fields if $s = 2$. In addition, $\tau = 2$ if $2\theta_B < \frac{\pi}{2}$ and $\tau = 1$ otherwise.

Using the standard methods of the dynamic theory [21], we can solve the following dispersion equation for X-ray waves propagating in the crystal, which is derived from system (3):

$$(\omega^2(1+\chi_0)-k^2)(\omega^2(1+\chi_0)-k_{\mathbf{g}}^2) - \omega^4\chi_{-\mathbf{g}}\chi_{\mathbf{g}}C^{(s)^2} = 0 \tag{7}$$

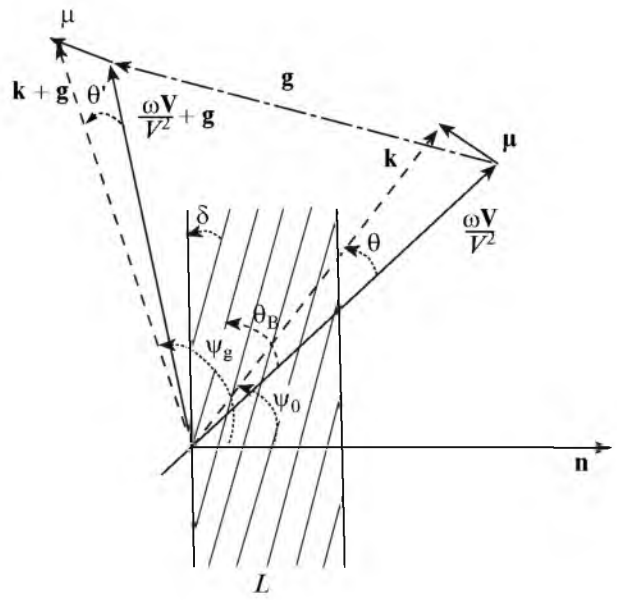

Fig. 1. Geometry of a radiation process: θ and θ' are the radiation angles, θ_B is the Bragg angle (an angle between electron velocity **V** and atomic planes), δ is the angle between the surface and atomic planes under consideration, and **k** and $\mathbf{k}_{\mathbf{g}}$ are, respectively, the wave vectors of incident and diffracted photons.

The projections of vectors **k** and $\mathbf{k}_{\mathbf{g}}$ are found as

$$\begin{aligned} k_x &= \omega\cos\psi_0 + \frac{\omega\chi_0}{2\cos\psi_0} + \frac{\lambda_0}{\cos\psi_0}, \\ k_{gx} &= \omega\cos\psi_{\mathbf{g}} + \frac{\omega\chi_0}{2\cos\psi_{\mathbf{g}}} + \frac{\lambda_{\mathbf{g}}}{\cos\psi_{\mathbf{g}}}. \end{aligned} \tag{8}$$

In this case, we use the known relationship between dynamic corrections λ_0 and $\lambda_{\mathbf{g}}$ [21]:

$$\lambda_{\mathbf{g}} = \frac{\omega\beta}{2} + \lambda_0\frac{\gamma_{\mathbf{g}}}{\gamma_0}, \tag{9}$$

Here, $\beta = \alpha - \chi_0\left(1 - \frac{\gamma_{\mathbf{g}}}{\gamma_0}\right)$, $\alpha = \frac{1}{\omega^2}(k_{\mathbf{g}}^2 - k^2)$, $\gamma_0 = \cos\psi_0$, $\gamma_{\mathbf{g}} = \cos\psi_{\mathbf{g}}$, ψ_0 is the angle between the wave vector **k** of an incident wave and the normal vector to the plate surface **n**, and $\psi_{\mathbf{g}}$ is the angle between wave vector $\mathbf{k}_{\mathbf{g}}$ and the normal vector. The values of vectors **k** and $\mathbf{k}_{\mathbf{g}}$ are

$$k = \omega\sqrt{1+\chi_0} + \lambda_0, \quad k_{\mathbf{g}} = \omega\sqrt{1+\chi_0} + \lambda_{\mathbf{g}}. \tag{10}$$

Assuming that $k_\parallel \approx \omega\sin\psi_0$ and $k_{\mathbf{g}\parallel} \approx \omega\sin\psi_{\mathbf{g}}$, we obtain

$$\lambda_0^{(1,2)} = \omega\frac{\gamma_0}{4\gamma_{\mathbf{g}}}\left(-\beta \pm \sqrt{\beta^2 + 4\chi_{\mathbf{g}}\chi_{-\mathbf{g}}C^{(s)^2}\frac{\gamma_{\mathbf{g}}}{\gamma_0}}\right), \tag{11a}$$

$$\lambda_{\mathbf{g}}^{(1,2)} = \frac{\omega}{4}\left(\beta \pm \sqrt{\beta^2 + 4\chi_{\mathbf{g}}\chi_{-\mathbf{g}}C^{(s)^2}\frac{\gamma_{\mathbf{g}}}{\gamma_0}}\right). \quad (11b)$$

Since $|\lambda_0| \ll \omega$ and $|\lambda_{\mathbf{g}}| \ll \omega$, the approximate equality $\theta \approx \theta'$ holds (Fig. 1) and, hence, θ' is used instead of θ below.

Under vacuum conditions, the solution to the first equation in system (3) for the incident field is written as

$$E_0^{(s)\mathrm{vac}\ I} = \frac{8\pi^2 ieV\theta P^{(s)}}{\omega}\frac{1}{-\chi_0 - \frac{2}{\omega}\lambda_0}\delta\left(\lambda_0^* - \lambda_0\right)$$
$$= \frac{8\pi^2 ieV\theta P^{(s)}}{\omega}\frac{1}{\frac{\gamma_0}{|\gamma_{\mathbf{g}}|}\left(-\chi_0 - \frac{2}{\omega}\frac{\gamma_0}{\gamma_{\mathbf{g}}}\lambda_{\mathbf{g}} + \beta\frac{\gamma_0}{\gamma_{\mathbf{g}}}\right)}\delta\left(\lambda_{\mathbf{g}}^* - \lambda_{\mathbf{g}}\right), \quad (12)$$

where $\lambda_{\mathbf{g}}^* = \frac{\omega\beta}{2} + \frac{\gamma_{\mathbf{g}}}{\gamma_0}\lambda_0^*$, $\lambda_0^* = \omega\left(\frac{\gamma^{-2} + \theta^2 - \chi_0}{2}\right)$,

$$\delta\left(\lambda_0^* - \lambda_0\right) = \frac{|\gamma_{\mathbf{g}}|}{\gamma_0}\delta\left(\lambda_{\mathbf{g}}^* - \lambda_{\mathbf{g}}\right).$$

The solutions to Eqs. (3) for the incident and diffracted fields of a crystal are written, respectively, as

$$E_0^{(s)\mathrm{cr}} = \frac{8\pi^2 ieV\theta P^{(s)}}{\omega}\frac{-\omega^2\beta - 2\omega\frac{\gamma_{\mathbf{g}}}{\gamma_0}\lambda_0}{4\frac{\gamma_{\mathbf{g}}}{\gamma_0}\left(\lambda_0 - \lambda_0^{(1)}\right)\left(\lambda_0 - \lambda_0^{(2)}\right)} \quad (13a)$$
$$\times\, \delta(\lambda_0 - \lambda_0^*) + E^{(s)^{(1)}}\delta(\lambda_0 - \lambda_0^{(1)}) + E^{(s)^{(2)}}\delta(\lambda_0 - \lambda_0^{(2)}),$$

$$E_{\mathbf{g}}^{(s)\mathrm{cr}} = \frac{8\pi^2 ieV\theta P^{(s)}}{\omega}\frac{\omega^2\chi_{\mathbf{g}}C^{(s,\tau)}}{4\frac{\gamma_0^2}{\gamma_{\mathbf{g}}^2}\left(\lambda_{\mathbf{g}} - \lambda_{\mathbf{g}}^{(1)}\right)\left(\lambda_{\mathbf{g}} - \lambda_{\mathbf{g}}^{(2)}\right)} \quad (13b)$$
$$\times\, \delta\left(\lambda_{\mathbf{g}}^* - \lambda_{\mathbf{g}}\right) + E^{(s)^{(1)}}\delta(\lambda_{\mathbf{g}} - \lambda_{\mathbf{g}}^{(1)}) + E^{(s)^{(2)}}\delta(\lambda_{\mathbf{g}} - \lambda_{\mathbf{g}}^{(2)}),$$

where $E^{(s)^{(1)}}$ and $E^{(s)^{(2)}}$ are the free fields corresponding to two solutions (11b) of dispersion equation (7).

Under vacuum conditions, the incident field and the diffracted field behind the crystal are defined, respectively, as

$$E_0^{(s)\mathrm{vac\ II}} = \frac{8\pi^2 ieV\theta P^{(s)}}{\omega}\frac{1}{-\chi_0 - \frac{2\lambda_0}{\omega}} \quad (14)$$
$$\times\, \delta(\lambda_0 - \lambda_0^*) + E_0^{(s)\mathrm{Rad}}\delta\left(\lambda_0 + \frac{\omega\chi_0}{2}\right),$$

$$E_{\mathbf{g}}^{(s)\mathrm{vac}} = E_{\mathbf{g}}^{(s)\mathrm{Rad}}\delta\left(\lambda_{\mathbf{g}} + \frac{\omega\chi_0}{2}\right), \quad (15)$$

where $E_0^{(s)\mathrm{Rad}}$ and $E_{\mathbf{g}}^{(s)\mathrm{Rad}}$ are the coherent radiation fields in the electron velocity direction and along the Bragg direction, respectively.

The diffracted and incident fields of a crystal are related by the expression following from the second equation in system (3):

$$E_0^{(s)\mathrm{cr}} = \frac{2\omega\lambda_{\mathbf{g}}}{\omega^2\chi_{\mathbf{g}}C^{(s,\tau)}}E_{\mathbf{g}}^{(s)\mathrm{cr}}. \quad (16)$$

To determine the amplitude of coherent radiations $E_0^{(s)\mathrm{Rad}}$ and $E_{\mathbf{g}}^{(s)\mathrm{Rad}}$, let us impose the ordinary boundary conditions on the input and output surfaces of the crystalline plate, which are written, respectively, as

$$\int E_0^{(s)\mathrm{vac}\ I}d\lambda_{\mathbf{g}} = \int E_0^{(s)\mathrm{cr}}d\lambda_{\mathbf{g}},$$
$$\int E_{\mathbf{g}}^{(s)\mathrm{cr}}d\lambda_{\mathbf{g}} = \int E_{\mathbf{g}}^{(s)\mathrm{vac}}d\lambda_{\mathbf{g}}, \quad (17a)$$
$$\int E_{\mathbf{g}}^{(s)\mathrm{cr}}\exp\left(i\frac{\lambda_{\mathbf{g}}}{\gamma_{\mathbf{g}}}L\right)d\lambda_{\mathbf{g}} = 0,$$

$$\int E_0^{(s)\mathrm{vac\ I}}d\lambda_0 = \int E_0^{(s)\mathrm{cr}}d\lambda_0,$$
$$\int E_0^{(s)cr}\,e^{i\frac{\lambda_0}{\gamma_0}L}\,d\lambda_0 = \int E_0^{(s)\mathrm{vac\ II}}\,e^{i\frac{\lambda_0}{\gamma_0}L}\,d\lambda_0, \quad (17b)$$
$$\int E_{\mathbf{g}}^{(s)\mathrm{cr}}\,e^{i\frac{\lambda_0}{\gamma_0}L}\,d\lambda_0 = 0.$$

For the coherent radiation fields, we obtain

$$E_{\mathbf{g}}^{(s)\mathrm{Rad}} = \frac{8\pi^2 ieV\theta P^{(s)}}{\omega}$$
$$\times\frac{\omega^2\chi_{\mathbf{g}}C^{(s,\tau)}\exp\left(i\left(\frac{\omega\chi_0}{2} + \lambda_{\mathbf{g}}^*\right)\frac{L}{\gamma_{\mathbf{g}}}\right)}{2\omega\left(\lambda_{\mathbf{g}}^{(2)}\exp\left(i\frac{\lambda_{\mathbf{g}}^* - \lambda_{\mathbf{g}}^{(2)}}{\gamma_{\mathbf{g}}}L\right) - \lambda_{\mathbf{g}}^{(1)}\exp\left(i\frac{\lambda_{\mathbf{g}}^* - \lambda_{\mathbf{g}}^{(1)}}{\gamma_{\mathbf{g}}}L\right)\right)}\times\left[\left(\frac{1}{\frac{\gamma_0}{|\gamma_{\mathbf{g}}|}\left(-\chi_0 - \frac{2}{\omega}\frac{\gamma_0}{\gamma_{\mathbf{g}}}\lambda_{\mathbf{g}}^* + \beta\frac{\gamma_0}{\gamma_{\mathbf{g}}}\right)} - \frac{2\omega\exp\left(i\frac{\lambda_{\mathbf{g}}^* - \lambda_{\mathbf{g}}^{(2)}}{\gamma_{\mathbf{g}}}L\right)}{4\frac{\gamma_0^2}{\gamma_{\mathbf{g}}^2}\left(\lambda_{\mathbf{g}}^* - \lambda_{\mathbf{g}}^{(1)}\right)}\right)\right.$$
$$\left.\times\left(1 - \exp\left(i\frac{\lambda_{\mathbf{g}}^* - \lambda_{\mathbf{g}}^{(1)}}{\gamma_{\mathbf{g}}}L\right)\right) - \left(\frac{1}{\frac{\gamma_0}{|\gamma_{\mathbf{g}}|}\left(-\chi_0 - \frac{2}{\omega}\frac{\gamma_0}{\gamma_{\mathbf{g}}}\lambda_{\mathbf{g}}^* + \beta\frac{\gamma_0}{\gamma_{\mathbf{g}}}\right)} - \frac{2\omega\exp\left(i\frac{\lambda_{\mathbf{g}}^* - \lambda_{\mathbf{g}}^{(1)}}{\gamma_{\mathbf{g}}}L\right)}{4\frac{\gamma_0^2}{\gamma_{\mathbf{g}}^2}\left(\lambda_{\mathbf{g}}^* - \lambda_{\mathbf{g}}^{(2)}\right)}\right)\left(1 - \exp\left(i\frac{\lambda_{\mathbf{g}}^* - \lambda_{\mathbf{g}}^{(2)}}{\gamma_{\mathbf{g}}}L\right)\right)\right], \quad (18)$$

$$E_0^{(s)\mathrm{Rad}} = \frac{8\pi^2 ieV\theta P^{(s)}}{\omega} \frac{\exp\left(i\left(\frac{\omega\chi_0}{2}+\lambda_0^*\right)\frac{L}{\gamma_0}\right)}{\lambda_{\mathbf{g}}^{(1)}\exp\left(i\frac{\lambda_0^{(2)}-\lambda_0^*}{\gamma_0}L\right)-\lambda_{\mathbf{g}}^{(2)}\exp\left(i\frac{\lambda_0^{(1)}-\lambda_0^*}{\gamma_0}L\right)}$$
$$\times\left[\lambda_{\mathbf{g}}^{(2)}\left(\frac{\omega}{-\omega\chi_0-2\lambda_0^*}+\frac{\omega}{2(\lambda_0^*-\lambda_0^{(2)})}\right)\left(1-\exp\left(i\frac{\lambda_0^{(2)}-\lambda_0^*}{\gamma_0}L\right)\right)\exp\left(i\frac{\lambda_0^{(1)}-\lambda_0^*}{\gamma_0}L\right)\right. \quad (19)$$
$$\left.-\lambda_{\mathbf{g}}^{(1)}\left(\frac{\omega}{-\omega\chi_0-2\lambda_0^*}+\frac{\omega}{2(\lambda_0^*-\lambda_0^{(1)})}\right)\times\left(1-\exp\left(i\frac{\lambda_0^{(1)}-\lambda_0^*}{\gamma_0}L\right)\right)\exp\left(i\frac{\lambda_0^{(2)}-\lambda_0^*}{\gamma_0}L\right)\right]$$

To perform subsequent analysis, it is convenient to represent $\lambda_0^{(1,2)}$, $\lambda_{\mathbf{g}}^{(1,2)}$, and $\lambda_{\mathbf{g}}^*$ as

$$\lambda_0^{(1,2)} = \frac{\omega\left|\chi_{\mathbf{g}}'C^{(s)}\right|}{2\varepsilon}\left(\xi^{(s)}-\frac{i\rho^{(s)}(1+\varepsilon)}{2}\right.$$
$$\left.\mp\sqrt{\xi^{(s)^2}-\varepsilon-i\rho^{(s)}((1+\varepsilon)\xi^{(s)}-2\kappa^{(s)}\varepsilon)-\rho^{(s)^2}\left(\frac{(1+\varepsilon)^2}{4}-\kappa^{(s)^2}\varepsilon\right)}\right), \quad (20a)$$

$$\lambda_{\mathbf{g}}^{(1,2)} = \frac{\omega\left|\chi_{\mathbf{g}}'C^{(s)}\right|}{2}\left(\xi^{(s)}-\frac{i\rho^{(s)}(1+\varepsilon)}{2}\right.$$
$$\left.\pm\sqrt{\xi^{(s)^2}-\varepsilon-i\rho^{(s)}((1+\varepsilon)\xi^{(s)}-2\kappa^{(s)}\varepsilon)-\rho^{(s)^2}\left(\frac{(1+\varepsilon)^2}{4}-\kappa^{(s)^2}\varepsilon\right)}\right), \quad (20b)$$

$$\lambda_{\mathbf{g}}^* = \frac{\omega\left|\chi_{\mathbf{g}}'C^{(s)}\right|}{2}\left(2\xi^{(s)}-i\rho^{(s)}-\varepsilon\sigma^{(s)}\right), \quad (21)$$

where

$$\xi^{(s)} = \xi^{(s)}(\omega) = \eta^{(s)}(\omega)+\frac{(1+\varepsilon)}{2\nu^{(s)}},$$
$$\nu^{(s)} = \frac{|\chi_{\mathbf{g}}'C^{(s)}|}{|\chi_0'|},\ \rho^{(s)} = \frac{\chi_0''}{|\chi_{\mathbf{g}}'C^{(s)}|},\ \varepsilon = \frac{|\gamma_{\mathbf{g}}|}{\gamma_0},\ \kappa^{(s)} = \frac{\chi_{\mathbf{g}}''C^{(s)}}{\chi_0''}$$
$$\eta^{(s)}(\omega) = \frac{\alpha}{2|\chi_{\mathbf{g}}'C^{(s)}|} \quad (22)$$
$$= \frac{2\sin^2\theta_{\mathrm{B}}}{V^2|\chi_{\mathbf{g}}'C^{(s)}|}\left(\frac{\omega_{\mathrm{B}}(1+\theta\cos\varphi\cot\theta_{\mathrm{B}})}{\omega}-1\right),$$
$$\sigma^{(s)} = \frac{1}{|\chi_{\mathbf{g}}'C^{(s)}|}\left(\theta^2+\gamma^{-2}-\chi_0'\right).$$

Since the inequality $2\sin^2\theta_{\mathrm{B}}/V^2|\chi_{\mathbf{g}}'C^{(s)}| \gg 1$, holds in the X-ray frequency range, $\eta^{(s)}(\omega)$ is the fast function of frequency ω. Hence, when the properties of PXR and diffracted transition radiation (DTR) will be analyzed below, it is convenient to accept $\eta^{(s)}(\omega)$ as a spectral variable characterizing frequency ω.. Note that the obtained formula involves $\eta^{(s)}(\omega)$, a $\xi^{(s)}(\omega) = \eta^{(s)}(\omega)+\frac{(1+\varepsilon)}{2\nu^{(s)}}$, where the second summand appears from the refraction effect, rather than $\gamma_{\mathbf{g}} = \cos\psi_{\mathbf{g}} < 0$. In derivation of formula (20), it was assumed that, in the radiation geometry under consideration, an angle between the diffracted photon momentum and the normal vector to the crystal surface is blunt. Therefore, $\gamma_{\mathbf{g}} = \cos\psi_{\mathbf{g}} < 0$.

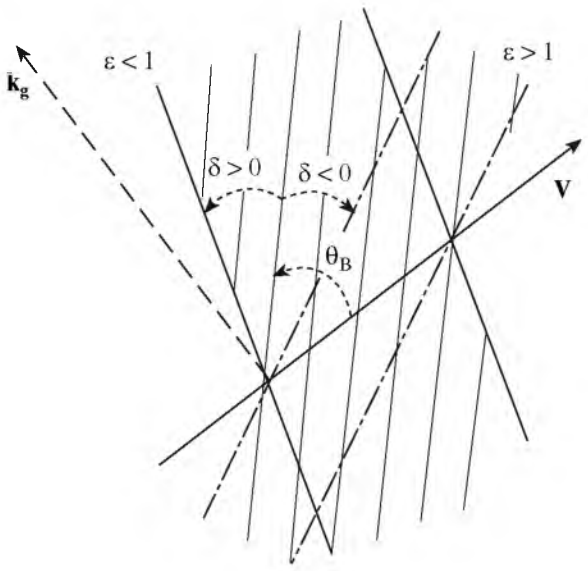

Fig. 2. Asymmetric (ε > 1, ε < 1) radiation reflections from the crystalline plate. In the case of ε = 1 (δ = 0), a symmetric reflection is observed.

Parameter ε in (20) can be represented as $\varepsilon = \sin(\theta_B - \delta)/\sin(\theta_B + \delta)$, where δ is an angle between the input surface of a target and a crystallographic plane. At a fixed value of θ_B, parameter ε determines the orientation of the input surface of a crystalline plate with respect to a set of diffracting atomic planes (Fig. 2). If the angle $(\theta_B + \delta)$ of electron incidence on a target decreases, parameter δ becomes negative (in the limiting case, $\delta \to -\theta_B$) and, subsequently, its absolute value grows, causing the value of ε to increase. If the angle of incidence increases, a decrease in ε is observed (in the limiting case, $\delta \to \theta_B$).

Parameter $\nu^{(s)}$ characterizes the degree of wave reflection from a set of parallel atomic planes in the crystal, which depends on the type (constructive $\left(\nu^{(s)} \approx 1\right)$ or destructive $\left(\nu^{(s)} \approx 0\right)$) of interference of waves reflected from atoms of different planes. Dynamic diffraction effects arise only when constructive interference occurs, i.e., owing to strong reflections of waves from a set of diffracting atomic planes of a crystal.

As is clear from formula (20a), there is a frequency range in which waves emitted near the input surface are completely reflected inside the crystal by atomic planes, not propagating forward. In this frequency range, the wave vector $k^{(1,2)} = \omega\sqrt{1+\chi_0} + \lambda_0^{(1,2)}$ has complex values even when there is no absorption $\left(\rho^{(s)} = 0\right)$, i.e., at the negative radicand of formula (20a). This frequency range is called the complete reflection region and defined as

$$\xi^{(s)^2} < \varepsilon \quad \text{or} \quad -\sqrt{\varepsilon} - \frac{1+\varepsilon}{2\nu^{(s)}} < \eta^{(s)} < \sqrt{\varepsilon} - \frac{1+\varepsilon}{2\nu^{(s)}}. \qquad (23)$$

Thus, the region width is determined by the value of $2\sqrt{\varepsilon}$.

SPECTRAL-ANGULAR RADIATION DENSITY IN THE BRAGG DIRECTION

Let us consider coherent radiation of a relativistic electron in the Bragg direction. Since PXR and DTR contribute to the radiation field, amplitude $E_{\mathrm{Rad}}^{(s)}$ can be represented as a sum of PXR and DTR amplitudes:

$$E_{\mathbf{g}}^{(s)\mathrm{Rad}} = E_{\mathrm{PXR}}^{(s)} + E_{\mathrm{DTR}}^{(s)}, \qquad (24a)$$

$$E_{\mathrm{PXR}}^{(s)} = \frac{8\pi^2 ieV\theta P^{(s)}}{\omega} \frac{\omega^2\chi_{\mathbf{g}}C^{(s,\tau)}\exp\left(i\left(\frac{\omega\chi_0}{2}+\lambda_g^*\right)\frac{L}{\gamma_g}\right)}{2\omega\left(\lambda_{\mathbf{g}}^{(2)}\exp\left(i\frac{\lambda_{\mathbf{g}}^* - \lambda_{\mathbf{g}}^{(2)}}{\gamma_{\mathbf{g}}}L\right) - \lambda_{\mathbf{g}}^{(1)}\exp\left(i\frac{\lambda_{\mathbf{g}}^* - \lambda_{\mathbf{g}}^{(1)}}{\gamma_{\mathbf{g}}}L\right)\right)}$$

$$\times\left[\left(\frac{2\omega\exp\left(i\frac{\lambda_{\mathbf{g}}^* - \lambda_{\mathbf{g}}^{(1)}}{\gamma_{\mathbf{g}}}L\right)}{4\frac{\gamma_0^2}{\gamma_{\mathbf{g}}^2}\left(\lambda_{\mathbf{g}}^* - \lambda_{\mathbf{g}}^{(2)}\right)} + \frac{\omega}{2\frac{\gamma_0}{|\gamma_{\mathbf{g}}|}\lambda_0^*}\right)\left(1 - \exp\left(i\frac{\lambda_{\mathbf{g}}^* - \lambda_{\mathbf{g}}^{(2)}}{\gamma_{\mathbf{g}}}L\right)\right)\right. \qquad (24b)$$

$$\left. - \left(\frac{2\omega\exp\left(i\frac{\lambda_{\mathbf{g}}^* - \lambda_{\mathbf{g}}^{(2)}}{\gamma_{\mathbf{g}}}L\right)}{4\frac{\gamma_0^2}{\gamma_{\mathbf{g}}^2}\left(\lambda_{\mathbf{g}}^* - \lambda_{\mathbf{g}}^{(1)}\right)} + \frac{\omega}{2\frac{\gamma_0}{|\gamma_{\mathbf{g}}|}\lambda_0^*}\right)\left(1 - \exp\left(i\frac{\lambda_{\mathbf{g}}^* - \lambda_{\mathbf{g}}^{(1)}}{\gamma_{\mathbf{g}}}L\right)\right)\right],$$

$$E_{\mathrm{DTR}}^{(s)} = \frac{8\pi^2 ieV\theta P^{(s)}}{\omega} \frac{\omega^2 \chi_g C^{(s,\tau)} \exp\left(i\left(\frac{\omega\chi_0}{2} + \lambda_g^*\right)\frac{L}{\gamma_g}\right)}{2\omega\left(\lambda_g^{(2)} \exp\left(-i\frac{\lambda_g^{(2)}}{\gamma_g}L\right) - \lambda_g^{(1)} \exp\left(-i\frac{\lambda_g^{(1)}}{\gamma_g}L\right)\right)}$$
$$\times \left[\frac{1}{\frac{\gamma_0}{|\gamma_g|}\left(-\chi_0 - \frac{2}{\omega}\frac{\gamma_0}{\gamma_g}\lambda_g^* + \beta\frac{\gamma_0}{\gamma_g}\right)} + \frac{\omega}{2\frac{\gamma_0}{|\gamma_g|}\lambda_0^*}\right]\left(\exp\left(-i\frac{\lambda_g^{(2)}}{\gamma_g}L\right) - \exp\left(-i\frac{\lambda_g^{(1)}}{\gamma_g}L\right)\right). \quad (24c)$$

Expression (24b) defines the PXR field amplitude, and (24c) describes the amplitude of the DTR field arising when transition radiation generated on the input surface is diffracted by a set of the atomic planes of a crystal. According to expression (24b), two branches of dispersion relationship (11) contributing to the PXR yield are possible, which correspond to two excited X-ray waves that are formed simultaneously with the equilibrium electromagnetic field of a fast particle.

Substituting (24b) into the known expression [22] for the spectral-angular density of X-rays,

$$\omega\frac{d^2N}{d\omega d\Omega} = \omega^2(2\pi)^{-6}\sum_{s=1}^{2}\left|E^{(s)\mathrm{Rad}}\right|^2 \quad (25)$$

and using (20), we obtain the expressions for the spectral-angular distribution of PXR:

$$\omega\frac{d^2N_{\mathrm{PXR}}^{(s)}}{d\omega d\Omega} = \frac{e^2}{\pi^2}\frac{P^{(s)^2}\theta^2}{(\theta^2 + \gamma^{-2} - \chi_0')^2}R_{\mathrm{PXR}}^{(s)}, \quad (26a)$$

$$R_{\mathrm{PXR}}^{(s)} = \left|\frac{\Omega_+^{(s)}}{\Delta^{(s)}}\frac{1-\exp\left(-ib^{(s)}\Delta_+^{(s)}\right)}{\Delta_+^{(s)}} - \frac{\Omega_-^{(s)}}{\Delta^{(s)}}\frac{1-\exp\left(-ib^{(s)}\Delta_-^{(s)}\right)}{\Delta_-^{(s)}}\right|^2. \quad (26b)$$

Here, the following designations are introduced:

$$\Delta^{(s)} = \left(\xi^{(s)} - K^{(s)} - i\rho^{(s)}\frac{1+\varepsilon}{2}\right)\exp\left(-ib^{(s)}\Delta_+^{(s)}\right) - \left(\xi^{(s)} + K^{(s)} - i\rho^{(s)}\frac{1+\varepsilon}{2}\right)\exp\left(-ib^{(s)}\Delta_-^{(s)}\right),$$
$$\Omega_\pm^{(s)} = \varepsilon\left((\sigma^{(s)} - i\rho^{(s)})\cdot\exp\left(-ib^{(s)}\Delta_\mp^{(s)}\right) + \Delta_\pm^{(s)}\right),$$
$$\Delta_\pm^{(s)} = \frac{\xi^{(s)} \pm K^{(s)}}{\varepsilon} - \sigma^{(s)} + i\frac{\rho^{(s)}(\varepsilon-1)}{2\varepsilon}, \quad (27)$$
$$K^{(s)} = \sqrt{\xi^{(s)^2} - \varepsilon - i\rho^{(s)}((1+\varepsilon)\xi^{(s)} - 2\kappa^{(s)}\varepsilon) - \rho^{(s)^2}\left(\frac{(1+\varepsilon)^2}{4} - \kappa^{(s)^2}\varepsilon\right)}, \quad b^{(s)} = \frac{\omega\left|\chi_g'\right|C^{(s)}}{2}\cdot\frac{L}{\gamma_0}.$$

Parameter $b^{(s)}$ is the ratio between the half path $L/(2\gamma_0)$ of an electron in the crystal and X-ray extinction length $\frac{1}{\omega\left|\chi_g' C^{(s)}\right|}$. in the crystal. Function $R_{\mathrm{PXR}}^{(s)}$ describes the PXR spectrum.

Let us consider a thin target $\left(b^{(s)}\rho^{(s)} \ll 1\right)$, In this case, absorption coefficient $\rho^{(s)}$ can be neglected. To observe the dynamic effects, we consider a crystal having a thickness within which the electron path length in the plate $(L/\sin(\delta - \theta_B))$ is many times greater that the X-ray extinction length $L_{ext}^{(s)} = \frac{1}{\omega\left|\chi_g' C^{(s)}\right|}$, In this case, expression (26b) describing the PXR spectrum is written as

$$R_{\mathrm{PXR}}^{(s)} = R_{\mathrm{PXR}}^{(1)^{(s)}} + R_{\mathrm{PXR}}^{(2)^{(s)}} + R_{\mathrm{PXR}}^{(\mathrm{INT})^{(s)}} \quad (28a)$$

$$R_{\mathrm{PXR}}^{(1)(s)} = \frac{\left(\xi^{(s)} - \sqrt{\xi^{(s)^2} - \varepsilon}\right)^2}{\xi^{(s)^2} - \varepsilon + \varepsilon \sin^2\left(\dfrac{b^{(s)}\sqrt{\xi^{(s)^2} - \varepsilon}}{\varepsilon}\right)} \frac{\sin^2\left(\dfrac{b^{(s)}}{2}\left(\dfrac{\xi^{(s)} - \sqrt{\xi^{(s)^2} - \varepsilon}}{\varepsilon} - \sigma^{(s)}\right)\right)}{\left(\dfrac{\xi^{(s)} - \sqrt{\xi^{(s)^2} - \varepsilon}}{\varepsilon} - \sigma^{(s)}\right)^2}, \tag{28b}$$

$$R_{\mathrm{PXR}}^{(2)(s)} = \frac{\left(\xi^{(s)} + \sqrt{\xi^{(s)^2} - \varepsilon}\right)^2}{\xi^{(s)^2} - \varepsilon + \varepsilon \sin^2\left(\dfrac{b^{(s)}\sqrt{\xi^{(s)^2} - \varepsilon}}{\varepsilon}\right)} \frac{\sin^2\left(\dfrac{b^{(s)}}{2}\left(\dfrac{\xi^{(s)} + \sqrt{\xi^{(s)^2} - \varepsilon}}{\varepsilon} - \sigma^{(s)}\right)\right)}{\left(\dfrac{\xi^{(s)} + \sqrt{\xi^{(s)^2} - \varepsilon}}{\varepsilon} - \sigma^{(s)}\right)^2}, \tag{28c}$$

$$R_{\mathrm{PXR}}^{(\mathrm{INT})(s)} = \frac{\varepsilon}{\xi^{(s)^2} - \varepsilon + \varepsilon \sin^2\left(\dfrac{b^{(s)}\sqrt{\xi^{(s)^2} - \varepsilon}}{\varepsilon}\right)} \frac{\cos\left(b^{(s)}\dfrac{\sqrt{\xi^{(s)^2} - \varepsilon}}{\varepsilon}\right)\left(\cos\left(b^{(s)}\left(\dfrac{\xi^{(s)}}{\varepsilon} - \sigma^{(s)}\right)\right) - \cos\left(b^{(s)}\dfrac{\sqrt{\xi^{(s)^2} - \varepsilon}}{\varepsilon}\right)\right)}{\left(\dfrac{\xi^{(s)}}{\varepsilon} - \sigma^{(s)}\right)^2 + \dfrac{\varepsilon - \xi^{(s)^2}}{\varepsilon^2}}. \tag{28d}$$

The PXR spectrum is represented as a sum of the spectra of two branches of excited X-ray waves ($R_{\mathrm{PXR}}^{(1)(s)}$ and $R_{\mathrm{PXR}}^{(2)(s)}$) and their interference summand $R_{\mathrm{PXR}}^{(\mathrm{INT})(s)}$.

SPECTRAL-ANGULAR RADIATION DENSITY ALONG THE EMITTING PARTICLE VELOCITY

Radiation field $E_0^{(s)\mathrm{Rad}}$ contains the contributions of FPXR and transition radiation (TR). Since experimental investigations of FPXR are hampered mainly by the interfering influence of the TR background. It is very important to represent amplitude $E_0^{(s)\mathrm{Rad}}$ as a sum of FPXR and TR amplitude:

$$E_0^{(s)\mathrm{Rad}} = E_{\mathrm{FPXR}}^{(s)} + E_{\mathrm{TR}}^{(s)}, \tag{29a}$$

$$E_{\mathrm{FPXR}}^{(s)} = \frac{8\pi^2 ieV\theta P^{(s)}}{\omega} \frac{\omega}{2\lambda^*} \frac{\exp\left(i\left(\dfrac{\omega\chi_0}{2} + \lambda_0^*\right)\dfrac{L}{\gamma_0}\right)}{\lambda_{\mathbf{g}}^{(1)} \exp\left(i\dfrac{\lambda_0^{(2)} - \lambda_0^*}{\gamma_0}L\right) - \lambda_{\mathbf{g}}^{(2)} \exp\left(i\dfrac{\lambda_0^{(1)} - \lambda_0^*}{\gamma_0}L\right)} \tag{29b}$$

$$\times \left[\frac{\lambda_{\mathbf{g}}^{(2)}\lambda_0^{(2)}}{\lambda_0^* - \lambda_0^{(2)}}\left(1 - \exp\left(i\frac{\lambda_0^{(2)} - \lambda_0^*}{\gamma_0}L\right)\right)\exp\left(i\frac{\lambda_0^{(1)} - \lambda_0^*}{\gamma_0}L\right) - \frac{\lambda_{\mathbf{g}}^{(1)}\lambda_0^{(1)}}{\lambda_0^* - \lambda_0^{(1)}}\left(1 - \exp\left(i\frac{\lambda_0^{(1)} - \lambda_0^*}{\gamma_0}L\right)\right)\exp\left(i\frac{\lambda_0^{(2)} - \lambda_0^*}{\gamma_0}L\right)\right],$$

$$E_{\mathrm{TR}}^{(s)} = \frac{8\pi^2 ieV\theta P^{(s)}}{\omega}\exp\left(i\left(\frac{\omega\chi_0}{2} + \lambda_0^*\right)\frac{L}{\gamma_0}\right)\left(\frac{\omega}{\omega\chi_0 + 2\lambda_0^*} - \frac{\omega}{2\lambda_0^*}\right)$$

$$\times \left(1 - \frac{\dfrac{\gamma_{\mathbf{g}}}{\gamma_0}(\lambda_0^{(1)} - \lambda_0^{(2)})\exp\left(i\dfrac{\lambda_0^{(2)} + \lambda_0^{(1)} - 2\lambda_0^*}{\gamma_0}L\right)}{\lambda_{\mathbf{g}}^{(1)} \exp\left(i\dfrac{\lambda_0^{(2)} - \lambda_0^*}{\gamma_0}L\right) - \lambda_{\mathbf{g}}^{(2)} \exp\left(i\dfrac{\lambda_0^{(1)} - \lambda_0^*}{\gamma_0}L\right)}\right). \tag{29c}$$

Substituting (29b) into (25) and using (20), we obtain the expressions describing the spectral-angular density of FPXR in a thin nonabsorbing crystal:

$$\omega\frac{d^2N^{(s)}_{\mathrm{FPXR}}}{d\omega d\Omega}=\frac{e^2}{\pi^2}\frac{P^{(s)^2}\theta^2}{(\theta^2+\gamma^{-2}-\chi_0')^2}R^{(s)}_{\mathrm{FPXR}}, \tag{30a}$$

$$R^{(s)}_{\mathrm{FPXR}}=R^{(1)^{(s)}}_{\mathrm{FPXR}}+R^{(2)^{(s)}}_{\mathrm{FPXR}}+R^{(\mathrm{INT})^{(s)}}_{\mathrm{FPXR}}, \tag{30b}$$

$$R^{(1)^{(s)}}_{\mathrm{FPXR}}=\frac{1}{\xi^{(s)^2}-\varepsilon+\varepsilon\sin^2\left(\dfrac{b^{(s)}\sqrt{\xi^{(s)^2}-\varepsilon}}{\varepsilon}\right)}\frac{\sin^2\left(\dfrac{b^{(s)}}{2}\left(\dfrac{\xi^{(s)}-\sqrt{\xi^{(s)^2}-\varepsilon}}{\varepsilon}-\sigma^{(s)}\right)\right)}{\left(\dfrac{\xi^{(s)}-\sqrt{\xi^{(s)^2}-\varepsilon}}{\varepsilon}-\sigma^{(s)}\right)^2}, \tag{30c}$$

$$R^{(2)^{(s)}}_{\mathrm{FPXR}}=\frac{1}{\xi^{(s)^2}-\varepsilon+\varepsilon\sin^2\left(\dfrac{b^{(s)}\sqrt{\xi^{(s)^2}-\varepsilon}}{\varepsilon}\right)}\frac{\sin^2\left(\dfrac{b^{(s)}}{2}\left(\dfrac{\xi^{(s)}+\sqrt{\xi^{(s)^2}-\varepsilon}}{\varepsilon}-\sigma^{(s)}\right)\right)}{\left(\dfrac{\xi^{(s)}+\sqrt{\xi^{(s)^2}-\varepsilon}}{\varepsilon}-\sigma^{(s)}\right)^2}, \tag{30d}$$

$$R^{(\mathrm{INT})^{(s)}}_{\mathrm{FPXR}}=\frac{1}{\xi^{(s)^2}-\varepsilon+\varepsilon\sin^2\left(\dfrac{b^{(s)}\sqrt{\xi^{(s)^2}-\varepsilon}}{\varepsilon}\right)}$$
$$\times\frac{\cos\left(b^{(s)}\dfrac{\sqrt{\xi^{(s)^2}-\varepsilon}}{\varepsilon}\right)\left(\cos\left(b^{(s)}\left(\dfrac{\xi^{(s)}}{\varepsilon}-\sigma^{(s)}\right)\right)-\cos\left(b^{(s)}\dfrac{\sqrt{\xi^{(s)^2}-\varepsilon}}{\varepsilon}\right)\right)}{\left(\dfrac{\xi^{(s)}}{\varepsilon}-\sigma^{(s)}\right)^2+\dfrac{\varepsilon-\xi^{(s)^2}}{\varepsilon^2}}. \tag{30e}$$

RATIO BETWEEN THE YIELDS OF PARAMETRIC AND FORWARD PARAMETRIC X-RAYS

The contribution of the second ((28c) and (30d)) and first ((28b) and (30c)) branches to the PXR and FPXR spectra is significant if the respective equations have solutions:

$$\frac{\xi^{(s)}(\omega)+\sqrt{\xi^{(s)}(\omega)^2-\varepsilon}}{\varepsilon}-\sigma^{(s)}=0, \tag{31}$$

$$\frac{\xi^{(s)}(\omega)-\sqrt{\xi^{(s)}(\omega)^2-\varepsilon}}{\varepsilon}-\sigma^{(s)}=0. \tag{32}$$

By solving Eqs. (31) and (32), we determine the central frequency of the spectrum of PXR photons emitted at the fixed angle of observation. Equations (31) and (32) indicate that the PXR spectrum maximum is always localized beyond the complete reflection (extinction) region:

$$\xi^{(s)}(\omega)=\sqrt{\varepsilon}+\frac{\left(\sigma^{(s)}\sqrt{\varepsilon}-1\right)^2}{2\sigma^{(s)}}>\sqrt{\varepsilon}, \tag{33}$$

Hence, in the case of a thin crystal, PXR and FPXR spectra are correctly described by formulas (28) and (30).

It can be shown that Eq. (31) has the solution if the condition

$$\varepsilon>\frac{1}{\sigma^{(s)^2}}\quad\text{or}\quad\varepsilon>\frac{\nu^{(s)^2}}{\left(\dfrac{\theta^2}{\left|\chi_0'\right|}+\dfrac{1}{\gamma^2\left|\chi_0'\right|}+1\right)^2}. \tag{34a}$$

is satisfied.

Equation (32) can be solved only if the condition

$$\varepsilon<\frac{1}{\sigma^{(s)^2}}\quad\text{or}\quad\varepsilon<\frac{\nu^{(s)^2}}{\left(\dfrac{\theta^2}{\left|\chi_0'\right|}+\dfrac{1}{\gamma^2\left|\chi_0'\right|}+1\right)^2}. \tag{34b}$$

holds.

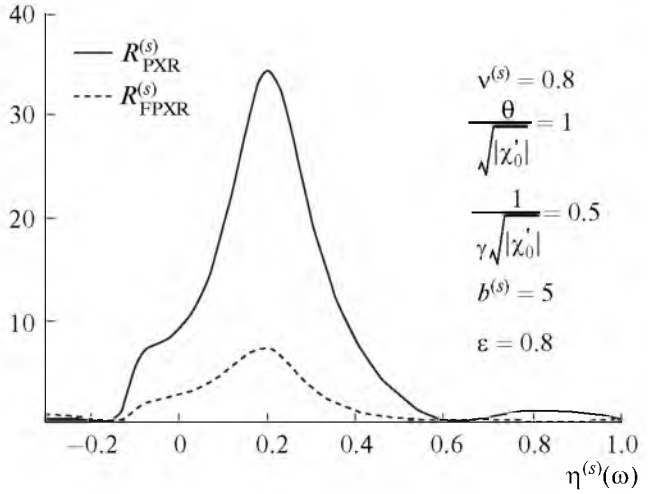

Fig. 3. PXR and FPXR spectra at the reflection asymmetry $\varepsilon = 0.8$.

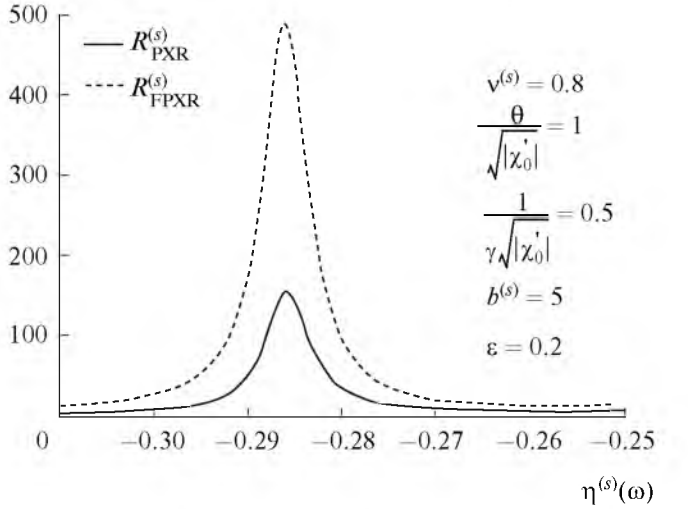

Fig. 4. PXR and FPXR spectra at the reflection asymmetry $\varepsilon = 0.2$.

The parameter $\nu^{(s)} = \frac{|\chi_g' C^{(s)}|}{|\chi_0'|}$ is close to unity; X-rays are strongly reflected by atomic planes, and its value is close to zero if weak reflections occur. Since $\nu^{(s)} < 1$, inequality (34a) is fulfilled solely when $\varepsilon \geq \nu^{(s)^2}$. In this case, only Eq. (31) is solvable and the PXR and FPXR yields are contributed by the second branch of the solution to the dispersion equation. For $\varepsilon < \nu^{(s)^2}$, the fulfillment of inequalities (34a) and (34b) is determined by observation angle θ and electron energy γ. Therefore, two branches of excited X-ray waves can contribute to the PXR and FPXR yields.

Since parameter ε affects the PXR and FPXR spectra described by respective quantities $R^{(s)}_{PXR}$ and $R^{(s)}_{FPXR}$, it is of interest to consider the influence of asymmetry on the ratio between the amplitudes of these spectra. Let us assume that inequality (34a) holds. Therefore, the second branch of PXR and FPXR provides the main contribution to the radiation yields. According to (28c) and (30d), the ratio of spectra is written as

$$\frac{R^{(2)^{(s)}}_{PXR}}{R^{(2)^{(s)}}_{FPXR}} = \left(\xi^{(s)} + \sqrt{\xi^{(s)^2} - \varepsilon}\right)^2. \qquad (35)$$

With allowance for (33), expression (35) implies that the PXR yield is much greater than the FPXR yield ($R^{(2)^{(s)}}_{PXR} \gg R^{(2)^{(s)}}_{FPXR}$) if $\varepsilon > 1$ and $\varepsilon \approx 1$. This fact is illustrated by the curves depicted in Fig. 3. Calculations were performed using formulas (28c) and (39d) and parameters presented in this figure. As might be expected, the PXR yield substantially exceeds the FPXR yield.

When asymmetry parameter ε decreases (i.e., if the angle of particle incidence on a target ($(\delta + \theta_B)$ in Fig. 2) increases), it follows from (35) that the PXR intensity at a small angle to the particle velocity can noticeably exceed the PXR intensity in the Bragg direction:

$$R^{(2)^{(s)}}_{PXR} \ll R^{(2)^{(s)}}_{FPXR}. \qquad (36)$$

as evidenced by the curves in Fig. 4. In this case, the PXR photon will leave from the plate at a small angle to its surface (Fig. 2).

Using Eq. (31) the solution to which is the frequency corresponding to concentration of the PXR photon spectrum in its neighborhood and the maximum of spectrum (33), it is possible to represent ratio (35) in the form

$$\frac{R^{(2)^{(s)}}_{PXR}}{R^{(2)^{(s)}}_{FPXR}} = \frac{\varepsilon^2}{\nu^{(s)^2}}\left(\frac{\theta^2}{|\chi_0'|} + \frac{1}{\gamma^2|\chi_0'|} + 1\right)^2. \qquad (37)$$

This ratio enables us to estimate the relative contribution of radiation, which depends on observation angle θ, the emitting particle energy determined by Lorenz factor γ, and parameter $\nu^{(s)}$. It follows from (37) that, at smaller angles of observation, the FPXR yield exceeds the PXR yield still more when the values of asymmetry parameter ε are small.

At the maximum of angular PXR density $\theta = \sqrt{\gamma^{-2} + |\chi_0'|}$, we obtain

$$\frac{R^{(2)^{(s)}}_{PXR}}{R^{(2)^{(s)}}_{FPXR}} = \frac{2\varepsilon^2}{\nu^{(s)^2}}\left(\frac{1}{\gamma^2|\chi_0'|} + 1\right)^2. \qquad (38)$$

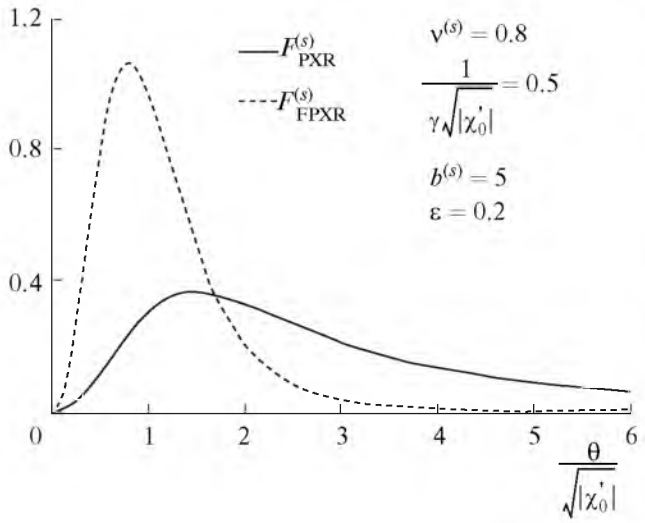

Fig. 5. Angular densities of PXR and FPXR at parameters identical to those in Fig. 4.

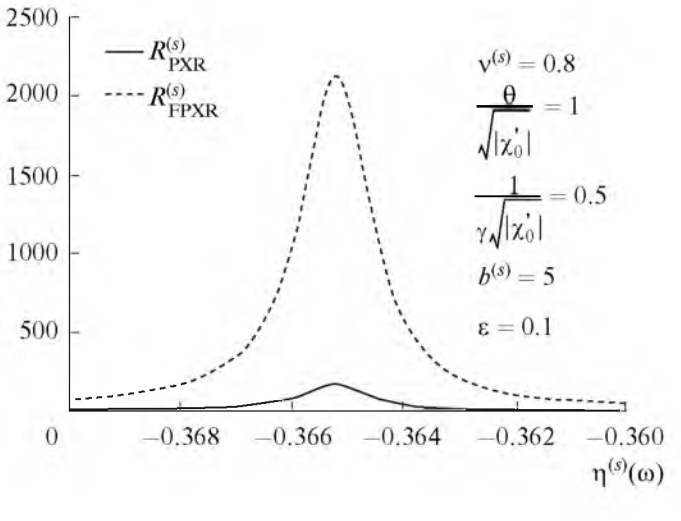

Fig. 6. PXR and FPXR spectra at the reflection asymmetry $\varepsilon = 0.1$.

Since the value of parameter $\nu^{(s)}$ is always less than unity, ratio (38) indicates that the PXR yield always exceeds the FPXR yield at $\gamma^2\left|\chi'_0\right| \ll 1$. The ratio of radiation yields substantially depends on asymmetry only if $\gamma^2\left|\chi'_0\right| \geq 1$.

Let us consider the influence of reflection asymmetry on the ratio of the angular densities of radiations. For this purpose, it is necessary to integrate expressions (26a) and (30a) over frequency functions $\eta^{(s)}(\omega)$:

$$\frac{dN^{(s)}_{PXR}}{d\Omega} = \frac{e^2 P^{(s)^2}}{2\pi^2 \sin^2\theta_B} F^{(s)}_{PXR}, \quad (39a)$$

$$F^{(s)}_{PXR} = \nu^{(s)} \frac{\frac{\theta^2}{\left|\chi'_0\right|}}{\left(\frac{\theta^2}{\left|\chi'_0\right|} + \frac{1}{\gamma^2\left|\chi'_0\right|} + 1\right)^2} \int_{-\infty}^{+\infty} R^{(s)}_{PXR}\, d\eta^{(s)}(\omega), \quad (39b)$$

$$\frac{dN^{(s)}_{FPXR}}{d\Omega} = \frac{e^2 P^{(s)^2}}{2\pi^2 \sin^2\theta_B} F^{(s)}_{FPXR}, \quad (40a)$$

$$F^{(s)}_{FPXR} = \nu^{(s)} \frac{\frac{\theta^2}{\left|\chi'_0\right|}}{\left(\frac{\theta^2}{\left|\chi'_0\right|} + \frac{1}{\gamma^2\left|\chi'_0\right|} + 1\right)^2} \int_{-\infty}^{+\infty} R^{(s)}_{FPXR}\, d\eta^{(s)}(\omega). \quad (40b)$$

Figure 5 presents the angular densities of PXR and FPXR constructed, respectively, from formulas (39b) and (40b) at $\gamma^2\left|\chi'_0\right| \geq 1$. The depicted curves indicate that the angular density of PXR along the emitting particle velocity still more exceeds the angular density of PXR.

Let us assume that inequality (34b) is fulfilled. Therefore, two branches can provide the contributions to the radiation yields, and the interference can be insignificant. In this case, according to (28b) and (30c), the ratio of PXR and FPXR spectra for the first branches of X-ray waves is written in the form

$$\frac{R^{(1)^{(s)}}_{PXR}}{R^{(1)^{(s)}}_{FPXR}} = \left(\xi^{(s)} - \sqrt{\xi^{(s)^2} - \varepsilon}\right)^2. \quad (41)$$

From comparison between (35) and (41), it is clear that the FPXR yield exceeds the PXR yield even more at small ε if the aforementioned inequality holds.

The fulfillment of inequality (34b) can ensure a decrease in asymmetry parameter ε. In connection with this, the FPXR spectrum amplitude is much greater than the PXR spectrum amplitude, as confirmed by the curves in Fig. 6. In this case, the main contribution is determined by the first branch $R^{(1)^{(s)}}_{FPXR}$ of PXR and interference summand $R^{(INT)^{(s)}}_{FPXR}$ (Fig. 7), and the angular density of FPXR still more exceeds the angular density of PXR, as demonstrated by curves in Fig. 8.

CONCLUSIONS

In this study, the analytical expressions for the spectral-angular radiation density along the emitting particle velocity and in the Bragg direction have been derived under the general condition of asymmetric reflections in the Bragg scattering geometry according to the two-wave approximation of the dynamic theory of diffraction. Analysis of the derived expressions has

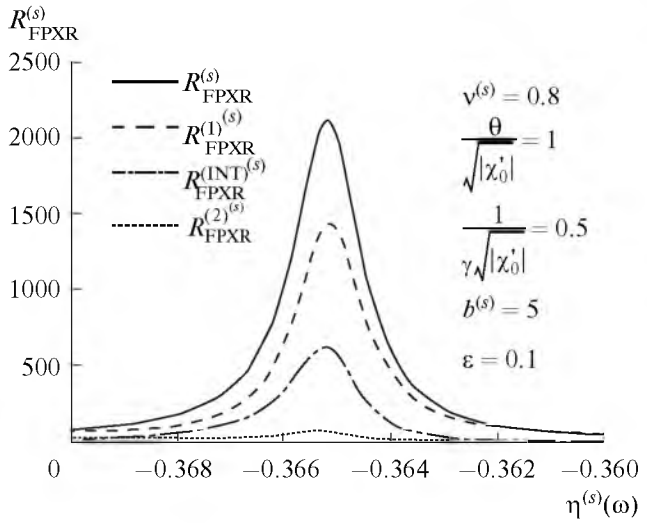

Fig. 7. Contributions of two branches and their interference summand to the PXR spectrum.

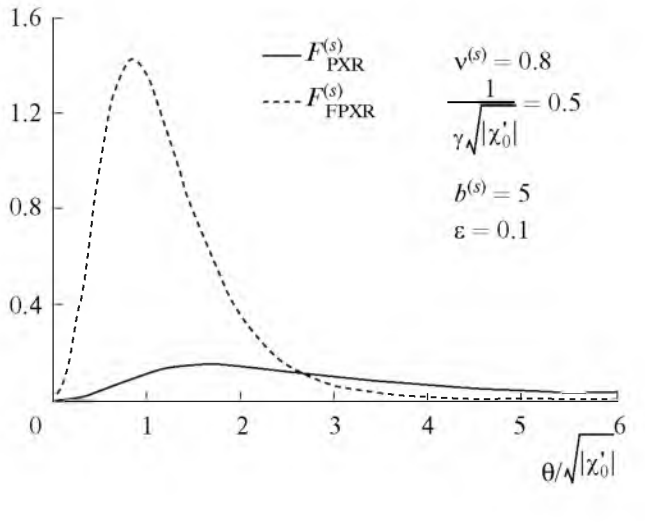

Fig. 8. Angular densities of PXR and FPXR at the reflection asymmetry $\varepsilon = 0.1$.

shown that the ratio of PXR and FPXR yields depends noticeably on the angle between diffracting atomic planes and the surface of a crystalline plate (δ) and, therefore, on reflection asymmetry parameter ε if the angle between the electron velocity and a set of diffracting atomic planes of a crystal (the Bragg angle θ_B) is fixed and the electron path in the crystalline plate ($2b^{(s)}$) remains unchanged.

A decrease in the parameter $\varepsilon = \sin(\delta - \theta_B)/\sin(\delta + \theta_B)$ (an increase in the angle $(\delta + \theta_B)$ of electron incidence on the crystalline plate) decreases the spectral-angular PXR density and increases the FPXR density, which begins exceeding the PXR density. In this case, each of the two branches of PXR and their interference can be substantial if asymmetry parameter $\varepsilon \ll 1$.

REFERENCES

1. M. L. Ter-Mikaelyan, *The Influence of the Medium on High-Energy Electromagnetic Processes* (AN ArmSSR, Yerevan, 1969) [in Russian].
2. G. M. Garibyan and Yan Shi, Zh. Eksp. Teor. Fiz. **61**, 930 (1971) [Sov. Phys. JETP **34**, 595 (1971)].
3. V. G. Baryshevskii and I. D. Feranchuk, Zh. Eksp. Teor. Fiz. **61**, 944 (1971) [Sov. Phys. JETP **34**, 502 (1971)].
4. G. M. Garibyan and Sh. Yan, Zh. Eksp. Teor. Fiz. **63**, 1198 (1972) [Sov. Phys. JETP **36**, 631 (1972)].
5. V. G. Baryshevsky and I. D. Feranchuk, Phys. Lett. A **57**, 183 (1976).
6. V. G. Baryshevsky and I. D. Feranchuk, J. Phys. (Paris) **44**, 913 (1983).
7. LukeC. L. Yuan, P. W. Alley, A. Bamberger, et al., Nucl. Instrum. Methods. Phys. Res. A **234**, 426 (1985).
8. B. N. Kalinin, G. A. Naumenko, D. V. Padalko, et al., Nucl. Instrum. Methods Phys. Res. B **173**, 253 (2001).
9. G. Kube, C. Ay, H. Backe, N. Clawiter, et al., in *Proceedings of the 5th Intern. Symposium on Radiation from Relativistic Electrons in Periodic Structures*, Lake Aya, Altai Mountains, Russia, 2001 (2001), p. 25.
10. H. Backe, N. Clawiter, Th. Doerk, et al., in *Proceedings of the Intern. Symposium on Channeling-Bent Crystals - Radiation Processes, 2003, Frankfurt am Main, Germany* (EP Systema Bt, Debrecen, 2003), p. 41.
11. A. N. Aleinik, A. N. Baldin, E. A. Bogomazova, et al., Pis'ma Zh. Eksp. Teor. Fiz. **80**, 447 (2004) [JETP Lett. **80**, 393 (2004)].
12. A. S. Kubankin, N. N. Nasonov, V. I. Sergienko, and I. E. Vnukov, Nucl. Instrum. Methods Phys. Res. A **201**, 97 (2003).
13. A. Kubankin, N. Nasonov, and A. Noskov, in *Proceedings of the 7th Intern. Russian-Japanese Symposium on Interaction of Fast Charged Particles with Solids* (Kyoto, Japan, 2002), p. 217.
14. N. Nasonov and A. Noskov, Nucl. Instrum. Methods Phys. Res. A **201**, 67 (2003).
15. S. V. Blazhevich and A. V. Noskov, Poverkhnost', No. 3, 62 (2008) [J. Surf. Invest. **2**, 225 (2008)].
16. S. V. Blazhevich and A. V. Noskov, Nucl. Instrum. Methods Phys. Res. A **266**, 3777 (2008).
17. S. V. Blazhevich and A. V. Noskov, Zh. Tekh. Fiz. **80** (3), 1 (2010) [Tech. Phys. **55**, 317 (2010)].
18. S. V. Blazhevich and A. V. Noskov, Poverkhnost', No. 6, 71 (2009).
19. S. V. Blazhevich and A. V. Noskov, Zh. Eksp. Teor. Fiz. **136**, 1043 (2009) [J. Exp. Theor. Phys. **109**, 901 (2009)].
20. S. V. Blazhevich and A. V. Noskov, Poverkhnost', No. 4, 40 (2010) [J. Surf. Invest. **4**, 303 (2010)].
21. Z. G. Pinsker, *Dynamical Scattering of X-rays in Crystals* (Nauka, Moscow, 1974; Springer, Berlin, 1978).
22. V. A. Bazylev and N. K. Zhivago, *Radiation from Fast Particles in Matter and External Fields* (Nauka, Moscow, 1987) [in Russian].